JPEDAV (2008) 29:11–19
DOI: 10.1007/s11669-007-9241-4
1547-7037 ©ASM International

Ternary Phase Equilibria at 450 °C in the Zn-Fe-P System

Zhi Li, Xuping Su, and Yuehui He

(Submitted February 23, 2007; in revised form June 19, 2007)

The 450 °C isothermal section of the Zn-Fe-P ternary phase diagram has been determined experimentally using optical microscopy, scanning electron microscopy (SEM) coupled with energy dispersive x-ray spectroscopy (EDS), and x-ray diffraction (XRD). The research of the work has concentrated on the Zn-rich corner, which is relevant to galvanizing. Experimental results indicate that P solubility in liquid zinc and all four Fe-Zn compounds, including ζ, δ, Γ_1, and Γ, is limited at 450 °C. Fe_2P is found to be in equilibrium with the ζ and δ phases. Fe_3P is found to be in equilibrium with δ, Γ_1, Γ, and αFe, respectively. Liquid Zn is in equilibrium with the Fe_2P and FeP phases.

Keywords phase equilibria, zinc-base alloy, Zn-Fe-P ternary system

1. Introduction

Zinc and zinc alloy coatings are widely used for improving the corrosion resistance of steels. Phosphorus is sometimes added to steel to improve its mechanical properties.[1] It is well known that the addition of phosphorus to interstitial-free (IF) steel can prevent denting of automotive steel.[2] In the galvanizing industry, steels that contain Si show that the thickness of a galvanized layer initially increases with increasing Si content to reach a maximum, after which the thickness decreases. This behavior is commonly known as the Sandelin effect.[3] Phosphorus in steel behaves in an analogous manner as has been shown by the work of Pelerin et al.[4], who studied the thickness of galvanized layers on steel as a function of phosphorus content of the steel.

The effect of phosphorus on the kinetics of coating formation during continuous galvanizing has been studied by many researchers.[2,5-8] Mercer[7] found that phosphorus segregated to the grain boundaries, impeded Fe and Zn interdiffusion, and lowered the amount of Fe that was found in galvanized coatings. Therefore, phosphorous in steel actually acts as an inhibitor to Fe-Zn alloy formation.[6,8,9] However, Lin et al.[10,11] thought that the phosphorous enrichment at the steel surface during recrystallization annealing retarded the formation and growth of Fe-Zn phases during the galvanizing process. Gladman et al.[12] studied the beneficial influence of phosphorus on the adhesion of galvanized layers on steels containing some silicon. If aluminum was added to a galvanizing bath, the work of Tobiyama and Kato[13] showed that the Al-rich layer formed during galvanizing was independent of either the phosphorus content of the steel or that in the galvanizing bath.

Currently available knowledge indicates that data concerning phase equilibria in the Zn-Fe-P ternary system is very important for understanding the effect of phosphorus on Fe-Zn reaction kinetics during galvanizing. Vogel and Horstmann[14] have determined an isothermal section of the Zn-Fe-P system at 750 °C. However, an isothermal section of the Zn-Fe-P system at temperatures relevant to hot dip galvanizing has not as yet been determined. In the present work, an isothermal section for the Fe-rich portion of the Zn-Fe-P system at 450 °C was established experimentally with techniques combining optical microscopy, scanning electron microscopy with energy dispersive x-ray spectroscopic capability (SEM-EDS), and x-ray diffraction.

2. Experimental Information for the Zn-Fe, Zn-P, and Fe-P Boundary Systems

Because of its importance to the galvanizing industry, the Zn-Fe binary system has been investigated repeatedly.[15-17] The most recent version was proposed by Su et al.[18] There are four compounds: ζ ($FeZn_{13}$), δ ($FeZn_{10}$), Γ_1 (Fe_5Zn_{21}), and Γ (Fe_3Zn_{10}), and they are shown in the phase diagram of Fig. 1(a).

Figure 1(b) shows the Zn-P phase diagram as compiled by Dutkiewicz,[19] but the P-rich side of the diagram is unknown, and only two compounds, Zn_3P_2 and ZnP_2, have been confirmed.

The Fe-P system is reported[20] to form five intermediate compounds: Fe_3P, Fe_2P, FeP, FeP_2, and FeP_4. However, the P-rich portion (P > 50%) of the diagram is undetermined

Zhi Li and **Yuehui He,** State Key Laboratory of Powder Metallurgy, Central South University, 410083 Changsha, Hunan, China; **Zhi Li** and **Xuping Su,** School of Mechanical Engineering, Xiangtan University, 411105 Xiangtan, Hunan, China. Contact e-mail: Yuehui@mail.csu.edu.cn.

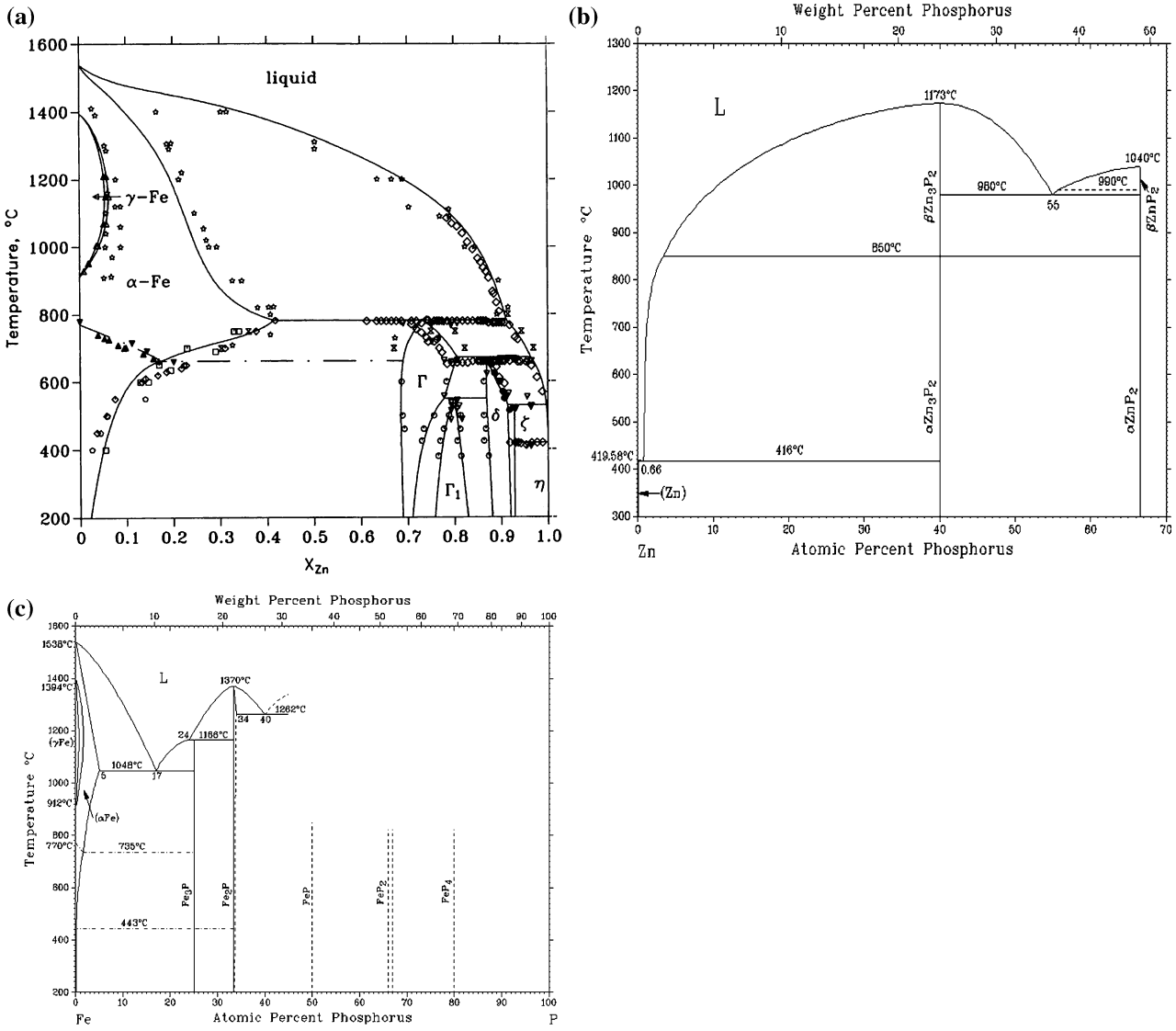

Fig. 1 (a) Zn-Fe binary system proposed by Su et al.[18] (b) Zn-P phase diagram. (c) Fe-P phase diagram

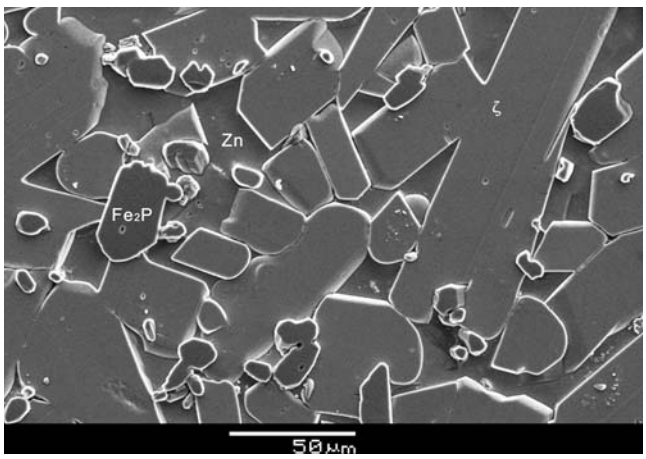

Fig. 2 Microstructure of Alloy P3. Three phases: ζ, η-(cph Zn), and Fe_2P

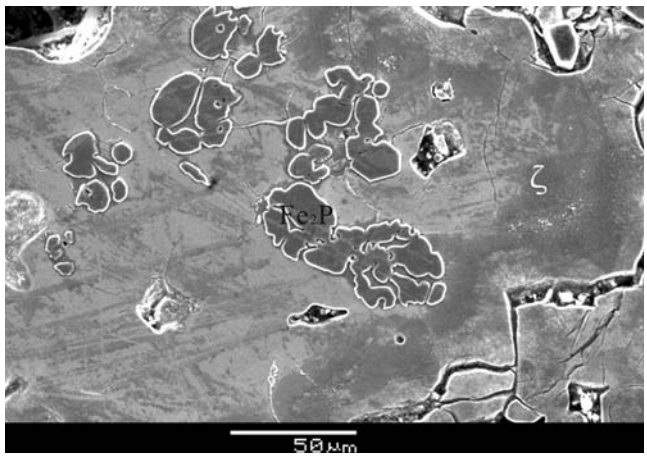

Fig. 3 Microstructure of Alloy P19. Two phases: ζ and Fe_2P

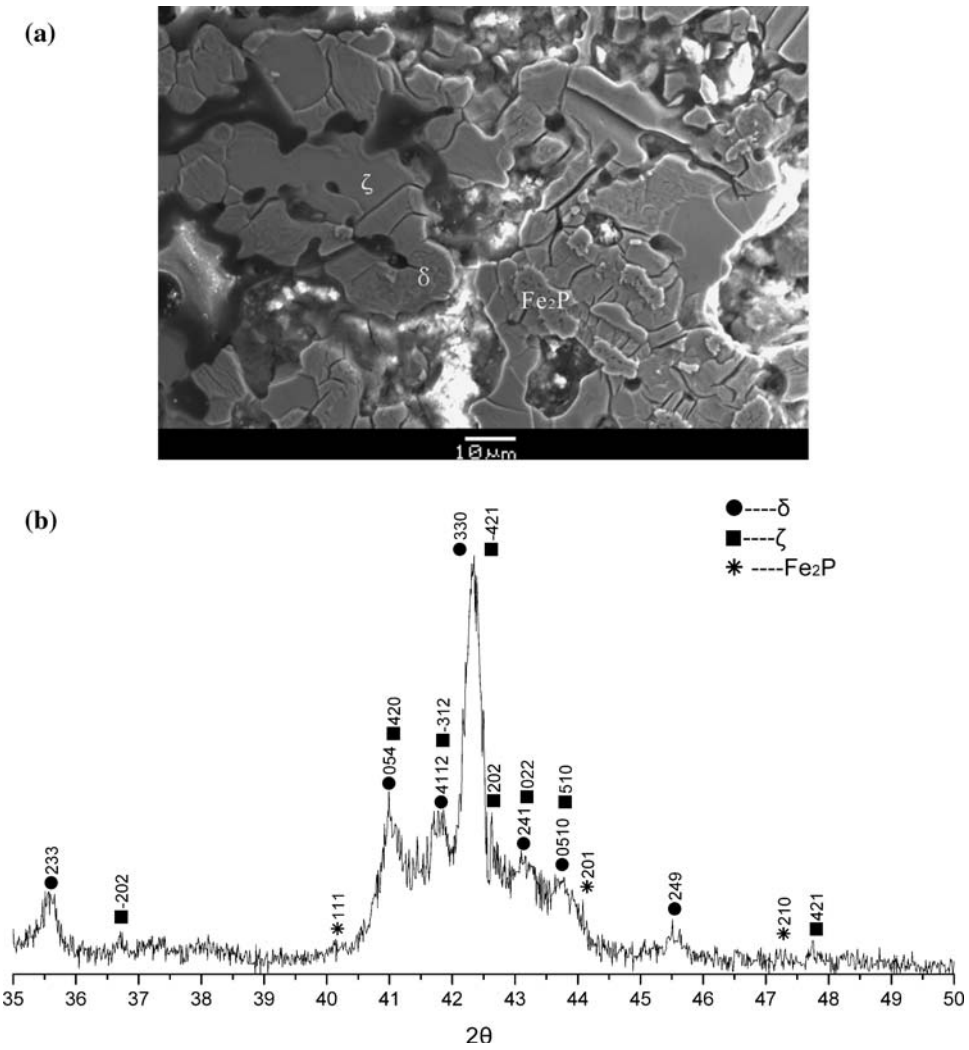

Fig. 4 Alloy P5. Three phases: ζ, δ, and Fe_2P. (a) Microstructure. (b) X-ray powder diffraction pattern

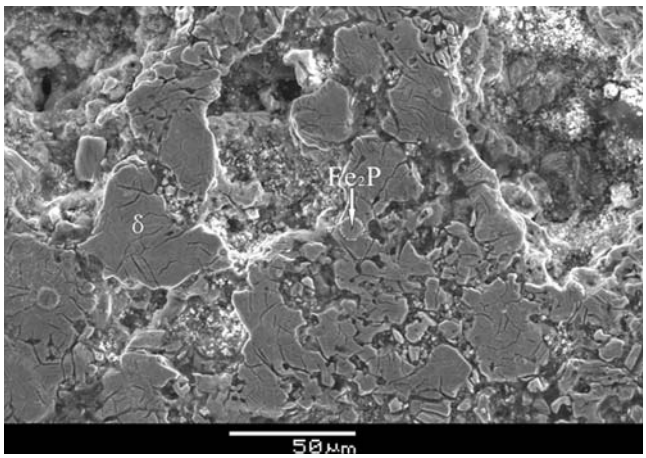

Fig. 5 The microstructure of Alloy P7. Two phases: δ and Fe_2P

because of the high volatility of phosphorus. The available data for the system are shown in Fig. 1(c).

3. Experimental Methods

In order to deduce the phase relationships in the Zn-Fe-P ternary system, a number of alloys were prepared from the elements with both Zn and Fe of 99.99% purity and P of 99.5% purity. For each sample, the three elements were mixed and sealed in an evacuated quartz tube. Each alloy mixture was heated to a temperature above its liquidus temperature and kept at this temperature for 2 days and was then quenched in water to minimize Zn loss and obtain a relatively compact sample. A bottom-quenching technique that has been reported in detail elsewhere[21] was used. The

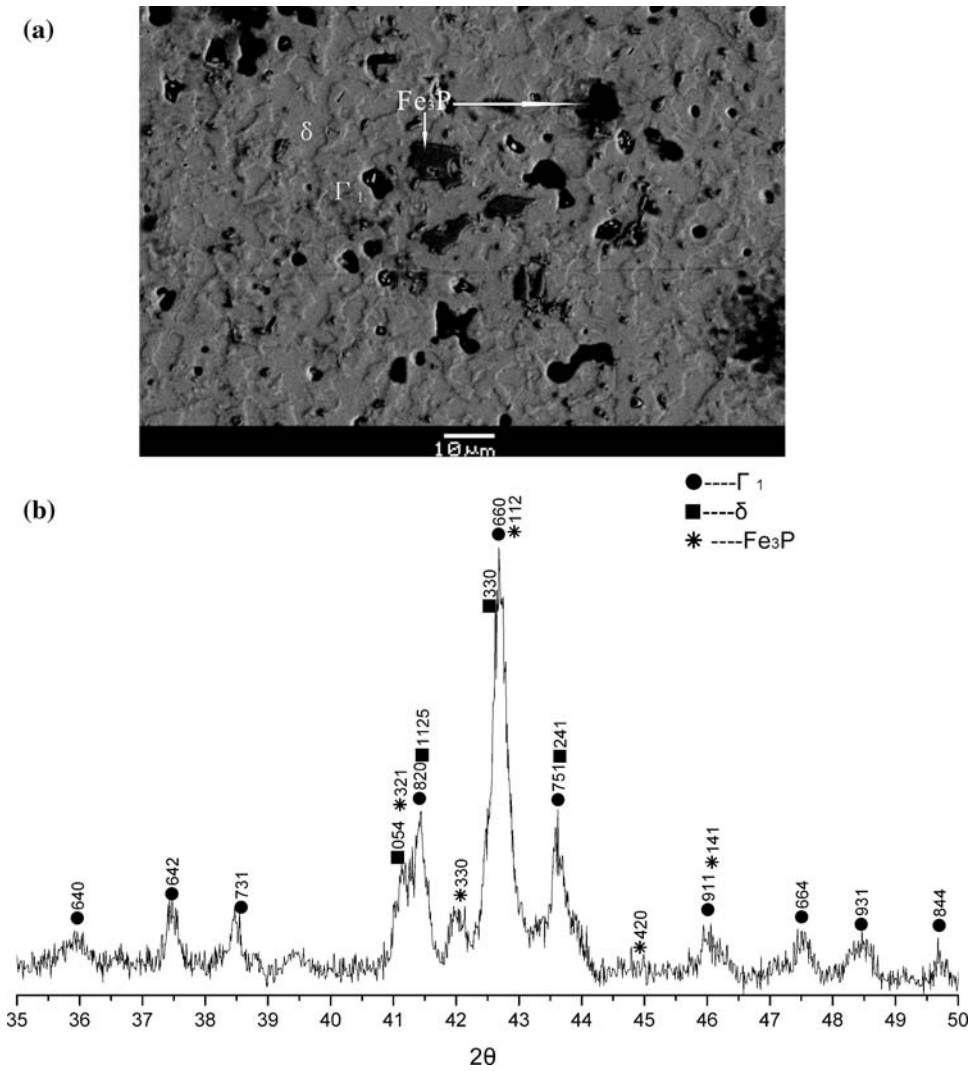

Fig. 6 Alloy P8. Three phases: Γ_1, δ, and Fe_3P. (a) Microstructure. (b) X-ray powder diffraction pattern

samples were sealed again and annealed at 450 °C for 60 days, then quenched into water at the end of the treatment. A nital etching solution was used for revealing microscopic details, and an optical microscope was used for the examination of all specimens. Structural studies of the alloys were performed using a D/max-rA x-ray diffractometer with Cu Kα radiation. SEM-EDS analyses were performed using a JSM-6360LV microscope to study the morphology and the chemical composition of the phases in the samples.

4. Results and Discussion

Forty samples were prepared for this study. Table 1 shows the nominal compositions of selected alloys in column 2, the phase in the alloys in column 3, and compositions determined by SEM-EDS in column 4. The compositions of the phases in column 4 are the averages of at least five measurements.

Examination of the microstructure of alloy P3 is shown in Fig. 2 and indicates that it consists of three phases. The SEM-EDS analyses suggest that the phases are ζ, Fe_2P, and η-(cph)Zn with the latter being in the liquid state at 450 °C. The microstructure of alloy P19 is shown in Fig. 3 and indicates that it is a two-phase mixture of ζ and Fe_2P phases. EDS analyses indicate the P content of the ζ and η-(cph)Zn phases is negligible.

A micrograph of alloy P5 is shown in Fig. 4(a) and indicates the presence of three phases. The x-ray diffraction of this alloy appears in Fig. 4(b) and identifies the three phases to be δ, ζ, and Fe_2P. The microstructure of alloy P7 is shown in Fig. 5, and the phases were identified as δ and

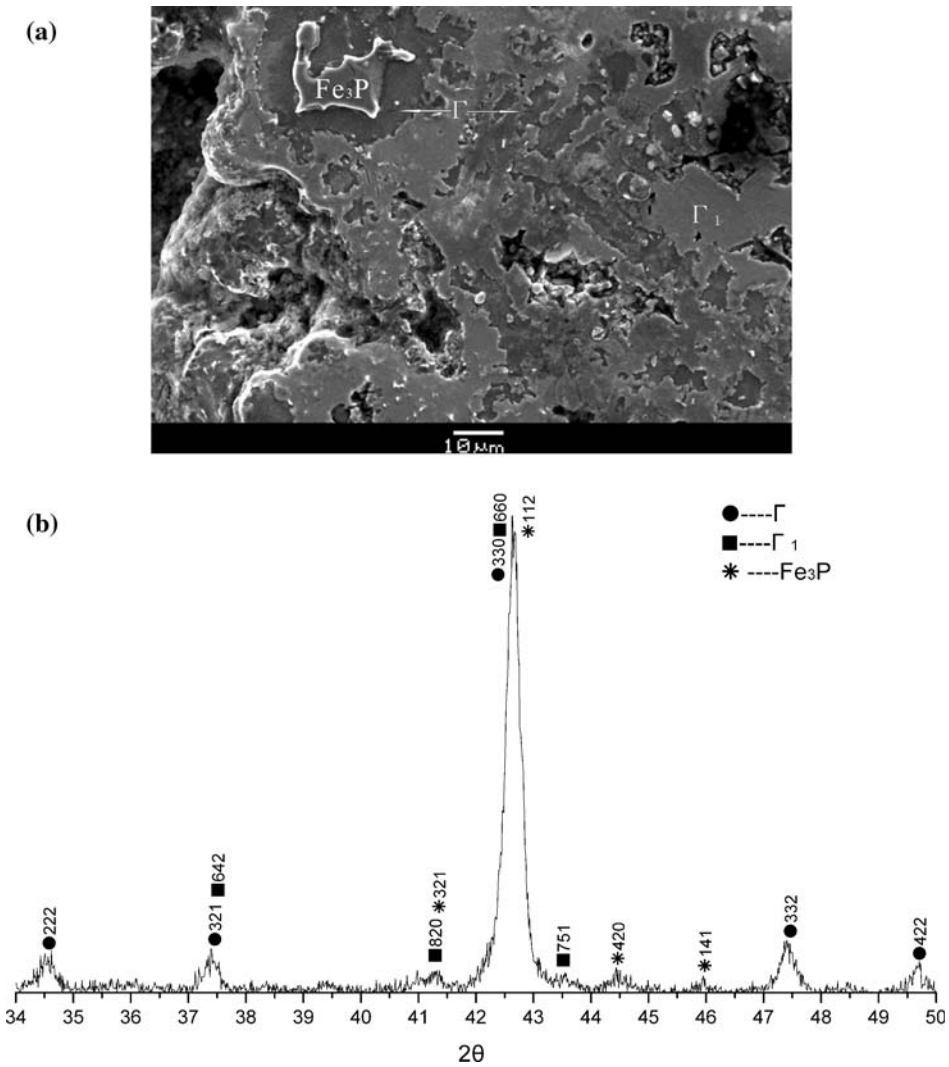

Fig. 7 Alloy P9. Three phases: Γ_1, Γ, and Fe_3P. (a) Microstructure. (b) X-ray powder diffraction pattern

Fe_2P. SEM-EDS analyses show the P solubility in the δ and Zn solubility in the Fe_2P phase to be undetectable and that the Fe to P ratio is near the ideal value of 2 to 1.

The microstructures and diffraction patterns are shown for alloy P8 in Fig. 6 and for alloy P9 in Fig. 7. The combined data show that the three alloy phases in P8 are Γ_1, δ, and Fe_3P, and in P9 the phases are Γ, Γ_1, and Fe_3P. EDS analyses indicate that the P solubilities in δ, Γ_1, and Γ phases are very limited. In the Fe_3P phase the atom ratio is again nearly ideal at 3 to 1 and Zn is undetectable.

Examination of the microstructure of alloy P10 in Fig. 8(a) shows the presence of three phases that were identified as FeP, Zn_3P_2, and η-(cph)Zn. The volume fraction of FeP in the alloy is too small to be resolved from the x-ray diffraction pattern that is shown in Fig. 8(b). Alloy P12 contains FeP, Fe_2P, and η-(cph)Zn, and the microstructure of this alloy is shown in Fig. 9. From the data in Table 1 it can be seen that the ratio of Fe to P in FeP is about 1 to 1 and of Zn to P in Zn_3P_2 is about 3 to 2.

The microstructure and x-ray diffraction pattern of alloy P26 in Fig. 10 indicate that the alloy contains three phases: αFe, Γ, and Fe_3P. As shown in Table 1, P solubility in αFe and Γ is also very limited. Figure 11 shows the x-ray diffraction pattern from alloy P29. This pattern clearly indicates that this alloy contains δ, Fe_2P, and Fe_3P.

When P > 50 at.%, samples are very difficult to prepare because of the high volatility of P. An attempt to determine the P-rich (P > 50 at.%) of the Zn-Fe-P system failed.

After examining the experimental results for all alloys, it was found that in no case was Zn detected in FeP, Fe_2P, or Fe_3P. The atomic ratios of these compounds were

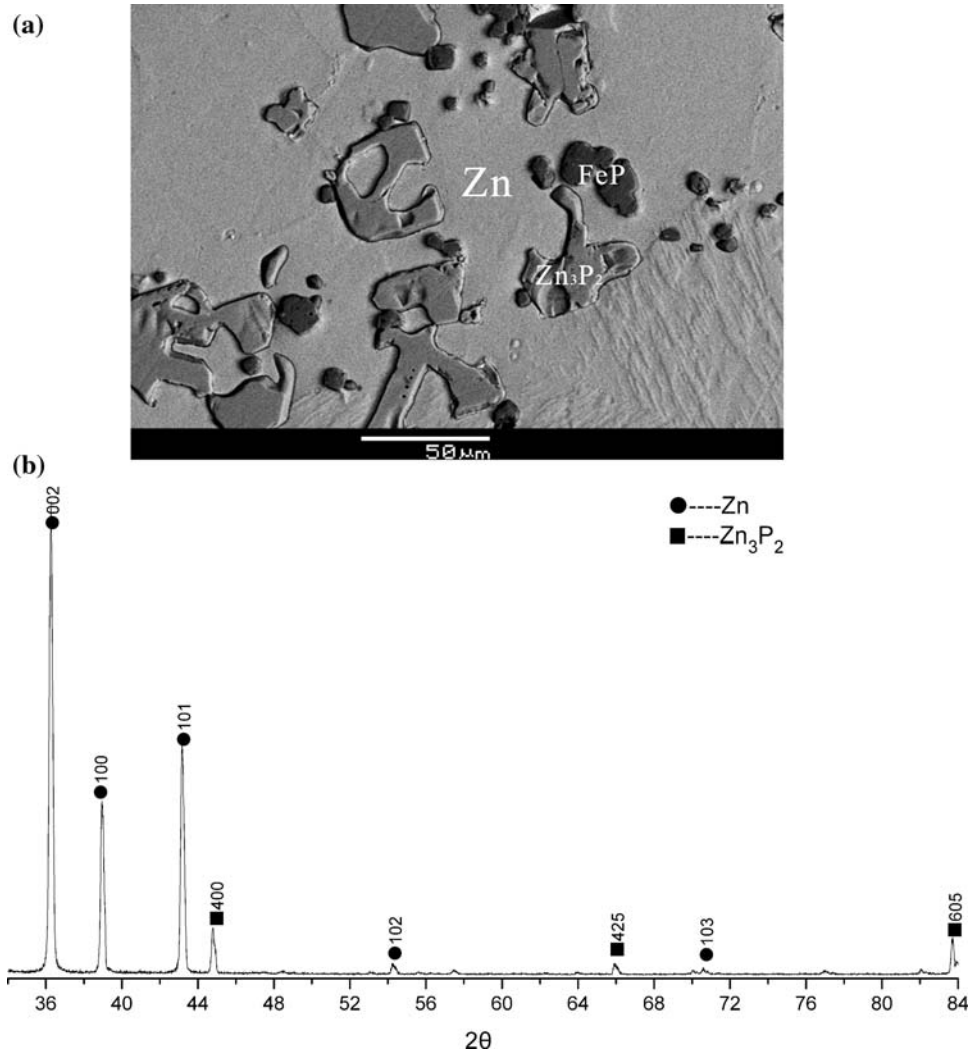

Fig. 8 Alloy P10. Three phases: FeP, Zn_3P_2, and η-(cph Zn). (a) Microstructure. (b) X-ray powder diffraction

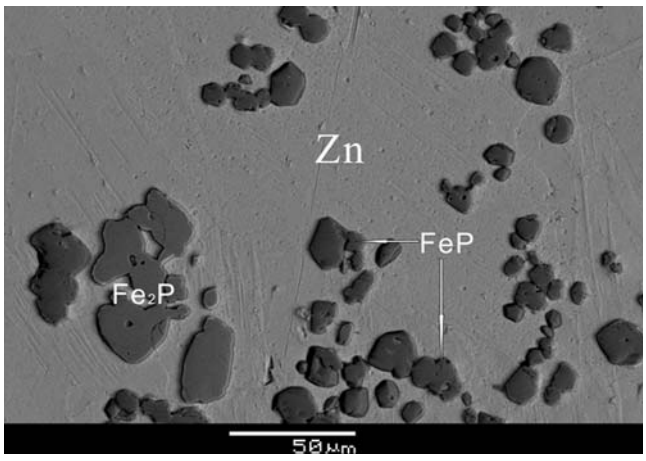

Fig. 9 Microstructure of Alloy P12. Three phases: FeP, Fe_2P and η-(cph Zn)

consistently found to be about 1 to 1, 2 to 1, and 3 to 1, respectively. Accordingly, these three phases are treated herein as stoichiometric compounds. EDS analyses have shown that P solubilities in all four Fe-Zn compounds, ζ, δ, Γ_1, and Γ, are limited at 450 °C. The compositions of these four phases in the ternary alloys are closely comparable to the compositions in the binary alloys.

Information from SEM-EDS analyses and x-ray diffraction patterns for the foregoing alloys were combined with data for the binary boundary phase diagrams to propose the partial 450 °C isothermal section of the ternary Zn-Fe-P phase diagram for the composition region where P < 50 at.%. This partial section is shown in Fig. 12. In this section there are eight three-phase fields with no indication of a ternary compound. These three-phase fields are: ζ + Liq Zn + Fe_2P, ζ + δ + Fe_2P, δ + Γ_1 + Fe_3P, Γ + Γ_1 + Fe_3P, Liq Zn + Zn_3P_2 + FeP, Liq Zn + Fe_2P + FeP, αFe + Γ + Fe_3P, and δ + Fe_3P + Fe_2P.

Table 1 Design compositions and phases of the alloys

Alloy	Design composition	Phase	at.% Fe	at.% Zn	at.% P
P3	Fe7Zn92.0P1	ζ	7.2	92.8	0
		Liq. Zn	0	100	0
		Fe_2P	Fe:P (at.%) ≈ 2:1		
P5	Fe9Zn90.25P0.75	ζ	7.5	92.5	0
		δ	9.2	90.8	0
		Fe_2P	Fe:P (at.%) ≈ 2:1		
P7	Fe12.8Zn85.7P1.5	δ	9.4	90.6	0
		Fe_2P	Fe:P (at.%) ≈ 2:1		
P8	Fe20Zn79P1	δ	14.5	85	0.5
		Γ_1	19.7	80.3	0
		Fe_3P	Fe:P (at.%) ≈ 3:1		
P9	Fe29Zn70P1	Γ	29.0	71.0	9
		Γ_1	22.1	77.9	0
		Fe_3P	Fe:P (at.%) ≈ 3:1		
P10	Fe1Zn93.5P5.5	Liq. Zn	0	100	0
		Zn_3P_2	0	59.5	40.5
		FeP	Fe:P (at.%) ≈ 1:1		
P12	Fe4Zn93P3	Liq. Zn	0	100	0
		Fe_2P	Fe:P (at.%) ≈ 2:1		
		FeP	Fe:P (at.%) ≈ 1:1		
P19	Fe10Zn87P3	ζ	7.3	92.7	0
		Fe_2P	Fe:P (at.%) ≈ 2:1		
P26	Fe44Zn53P3	αFe	92.7	7.3	0
		Γ	30.3	69.7	0
		Fe_3P	Fe:P (at.%) ≈ 3:1		
P29	Fe16Zn83P1	δ			
		Fe_3P			
		Fe_2P			

5. Conclusions

In this work, a partial ternary phase diagram at 450 °C has been determined for the Zn-Fe-P system in the region where P < 50 at.%, and the main findings are:

- There are eight three-phase regions in that portion of the Zn-Fe-P phase diagram lying below 50 at.% P.
- P solubility in liquid Zn and in the four Zn-Fe compounds is very limited at 450 °C, and the compositions of the ζ, δ, Γ_1, and Γ phases in ternary alloys are not significantly different from those of the binary system.
- Fe_2P was found to be in equilibrium with the ζ and δ phases, Fe_3P was found to be in equilibrium with δ, Γ_1, Γ, and αFe, respectively, and FeP was found in equilibrium with Zn_3P_2 and liquid Zn.

Acknowledgement

This investigation is supported by Hunan Provincial Natural Science Foundation (No. 05JJ40091) and National Natural Science Foundation of China (No. 50271059, No. 50671088).

References

1. A.R. Marder, A Review of the Metallurgy of Zinc Coated Steel, *Prog. Mater. Sci.*, 2000, **45**, p 191
2. C.E. Jordan, R. Zuhr, and A.R. Marder, Effect of Phosphorus Surface Segregation on Iron-Zinc Reaction Kinetics During Hot-Dip Galvanizing, *Metall. Mater. Trans. A*, 1997, **28A**, p 2695
3. R.W. Sandelin, Galvanizing Characteristics of Different Types of Steels, *Wire Wire Prod.*, 1940, **15**, p 655
4. J. Pelerin, J. Hoffmann, and V. Leroy, Metallwissenschaft Und Technik, 1981, **35**, p 870
5. T. Toki, K. Oshima, T. Nakamori, et al., *The Physical Metallurgy of Zinc Coated Steel*, A.R. Marder, Ed., TMS, Warrendale, PA, 1994, p 169
6. L. Allegra, R.G. Hart, and H.E. Townsend, Intergranular Zinc Embrittlement and Its Inhibition by Phosphorus in 55% Al-Zn-coated Steel Sheet, *Metall. Trans. A*, 1983, **14A**, p 401

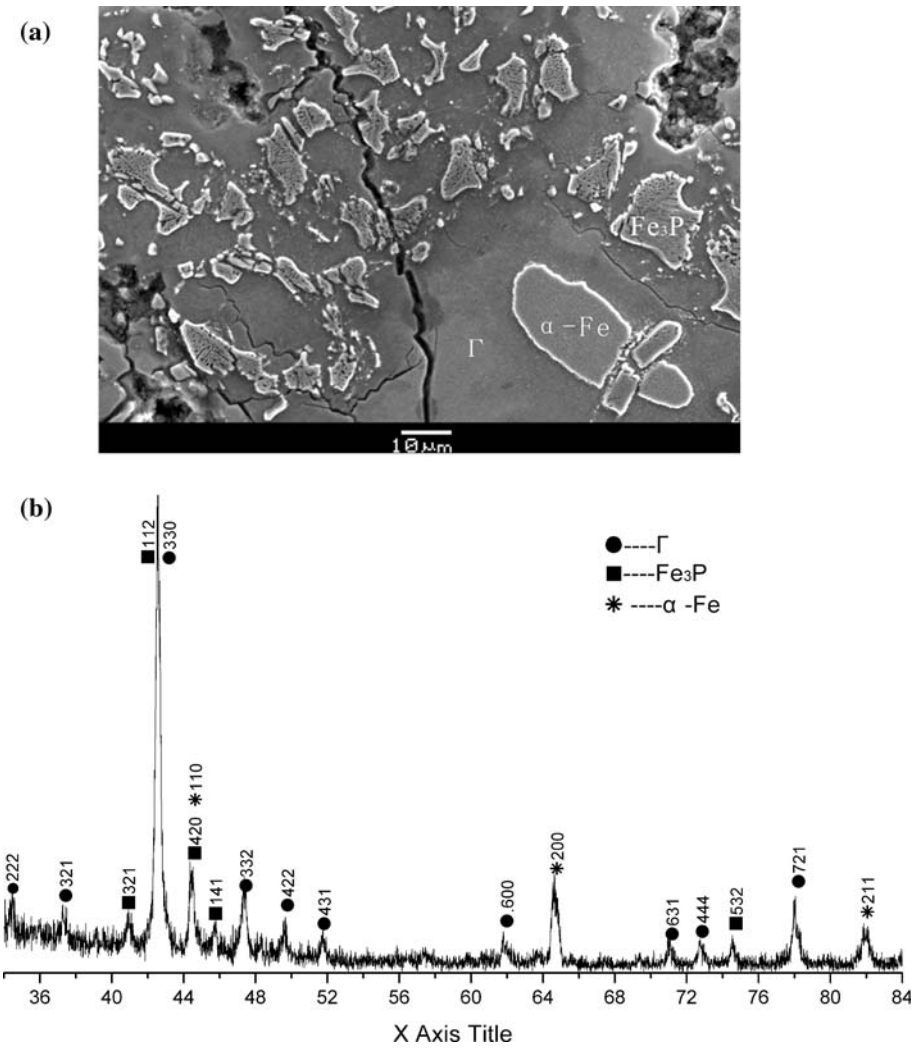

Fig. 10 Alloy P26. Three phases: αFe, Γ, and Fe_3P. (a) Microstructure. (b) X-ray powder diffraction pattern

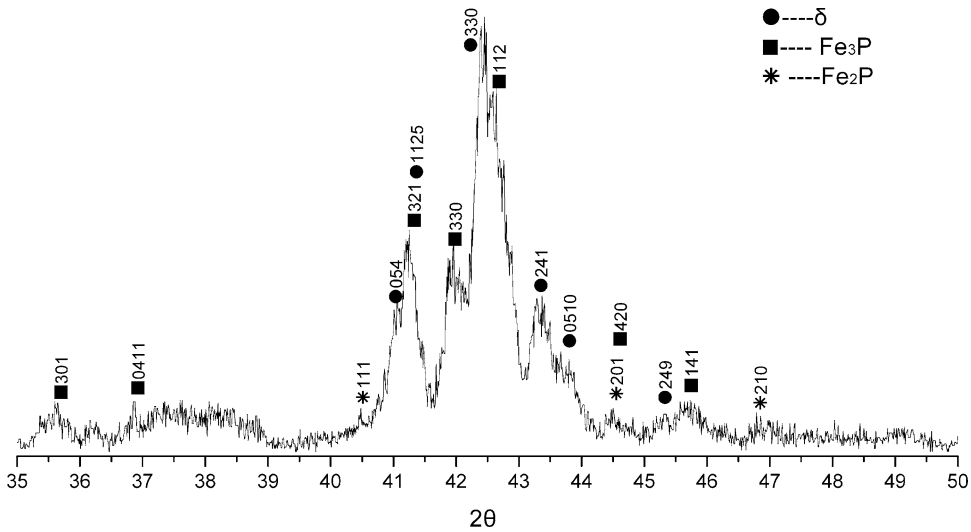

Fig. 11 X-ray powder diffraction pattern of alloy P29. Three phases: δ, Fe_2P, and Fe_3P

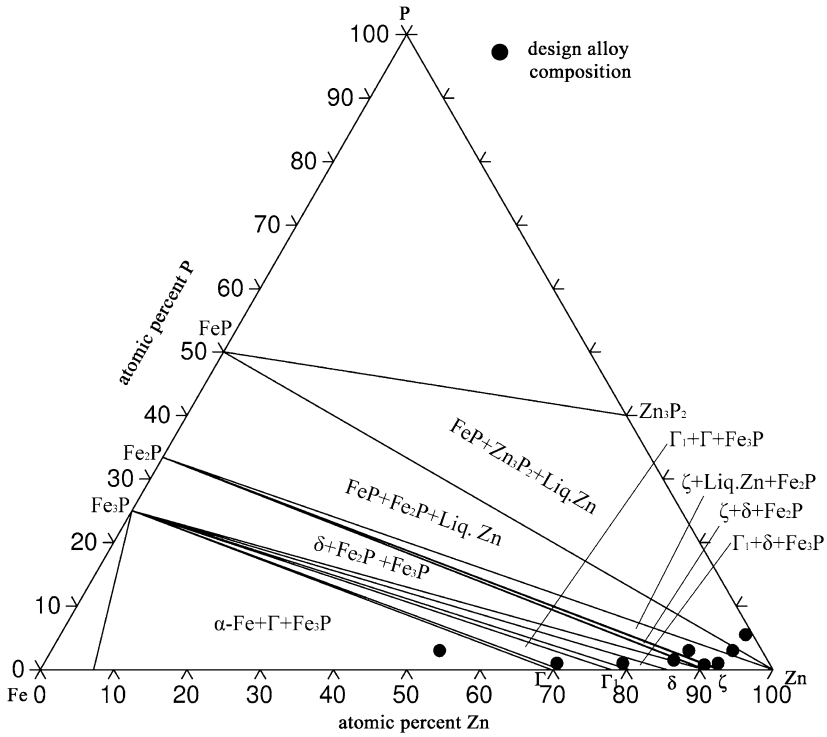

Fig. 12 The partial phase diagram of the Zn-Fe-P ternary system at 450 °C

7. J.D. Mercer, *Galvatech '92*. Verlag Stahl Eisen, Amsterdam, 1992, p 204
8. H. Yamaguchi and Y. Hisamatsu, *Trans. Iron Steel Inst. Jpn.*, 1979, **14,** p 649
9. M. Guttmann, Y. Lepretre, A. Aubry, M.-J. Roch, et al., Mechanisms of the Galvanizing Reaction. Influence of Titanium and Phosphorus Contents in Steel and of Its Surface Microstructure after Annealing,*Galvatech'95*, Iron and Steel Society, Warrendale, PA, 1995, p 295
10. C.S. Lin, W.A. Chou, and M. Meshii, Effect of Phosphorus Content in Base-Steel on the Formation of Alloy Layer of Hot-Dip Coated Steel Sheets, *The Physical Metallurgy of Zinc Coated Steel*, A.R. Marder, Ed., TMS, Warrendale, PA, 1994, p 31
11. C.S. Lin, M. Meshii, and C.C. Cheng, Phase Evolution in Galvanneal Coatings on Steel Sheets, *ISIJ Int.*, 1995, **35**, p 503
12. T. Gladman, B. Holmes, and F.B. Pickering, *JISI*, 1973, **211** (Part 11), p 765
13. Y. Tobiyama and C. Kato, Effect of the Substrate Compositions on the Growth of Fe-Al Interfacial Layer Formed During Hot Dip Galvanizing, *J. Iron Steel Inst. Jpn.*, 2003, **89**, p 38
14. R. Vogel and D. Horstmann, *Archiv. Eisenhüttenwes.*, 1953, **24,** p 247
15. J. Schramm, *Z. Metallkd.*, 1936, **28,** p 203
16. M. Hamalainen, R. Luoma, and P. Taskinen, "Thermodynamic Analysis of the System Iron-Lead-Zinc," Report TKK-V-B55, Helsinki University of Technology, Espoo, Finland, 1990
17. G. Reumont, P. Perrot, J.M. Fiorani, and J. Hertz, Thermodynamic Assessment of the Fe-Zn System, *J. Phase Equilibria*, 2000, **21**, p 371
18. X. Su, N.-Y. Tang, and J.M. Toguri, Thermodynamic Evaluation of the Fe-Zn System, *J. Alloys Compd.*, 2001, **325**, p 129
19. J. Dutkiewicz, P-Zn (Phosphorus-Zinc), *Binary Alloy Phase Diagrams*, T.B. Massalski, Ed., ASM International, Materials Park, OH, 1990, p 2995
20. H. Okamoto, Fe-P (Iron-Phosphorus), *Binary Alloy Phase Diagrams*, T.B. Massalski, Ed., ASM International, Materials Park, OH, 1990, p 1746
21. X.P. Su, N.-Y. Tang, and J.M. Toguri, 450 °C Isothermal Section of the Fe-Zn-Si Ternary Phase Diagram, *Can. Metall. Q.*, 2001, **40**, p 377